Evidence for human influence on climate from hemispheric temperature relations

Robert K. Kaufmann* & David I. Stern†

* Center for Energy and Environmental Studies, 675 Commonwealth Avenue, Boston University, Boston, Massachusetts 02215, USA
† Centre for Resource and Environmental Studies, Australian National University, Canberra ACT 0200, Australia

....

Analysis of observational temperature records for the Northern and Southern hemispheres indicates a statistical relationship in which Northern Hemisphere temperature depends on temperature in the Southern Hemisphere. This pattern, which has strengthened over time, can be explained by the climatic effects of anthropogenic trace gases and tropospheric sulphate aerosols. A similar statistical pattern is produced by model simulations of the historical atmosphere.

There is general agreement that the average surface air temperature of the Earth has increased by about 0.6 °C over the past century[1–3]. But the cause(s) of the temperature increase is (are) uncertain[4–6]: the increase may be caused by natural mechanisms, by human activity, or by both.

There is increasing evidence that some of the temperature increase can be attributed to activities that increase the atmospheric concentration of greenhouse gases and tropospheric sulphates[7]. Including these gases in atmospheres used in climate models increases these models' ability to simulate the spatial and temporal pattern of the historical temperature record[8]. Further evidence is provided by analysis of the historical temperature record using spectral analysis[9–11] or single equation regression models[9,12–15]. Some of these studies find that anthropogenic variables have a significant effect on global temperatures. Nonetheless, many of these results are difficult to interpret from either a statistical and/or a physical standpoint because there are no clear criteria for the selection of variables, and the specification of dynamic structure and/or the time-series properties of the variables have been ignored in deriving inferences. To alleviate these difficulties, we use here standard econometric time-series criteria for model selection, simulate the distributions of test statistics under different assumptions about the time-series properties of the variables, and search for similar results in the output of a coupled general circulation model (CGCM).

The analysis focuses on the spatial pattern of temperature change that may be generated by economic activities (which occur predominantly in the Northern Hemisphere) that increase the concentration of greenhouse gases globally, but which increase the concentration of tropospheric sulphates in the Northern Hemisphere relative to the Southern Hemisphere. This difference may allow us to attribute temperature change between 1865 and 1994 to economic activity by answering three questions: (1) is there a causal order to temperature changes in the Northern and Southern hemispheres; (2) what factors are responsible for the causal order; and (3) are hypotheses about the factors responsible for causal order consistent with the results generated by CGCMs.

Traditional regression or correlation analysis does not indicate whether the estimated relationship is coincidental or whether the 'dependent' variable is meaningfully dependent on changes in the 'independent' variables. This type of dependence can be examined by testing for Granger causality[16]. The presence of Granger causality implies the presence of a statistical causal ordering. Granger causality tests are based on the notion of predictability, in particular whether past values of a variable X contain statistically meaningful information about current values of variable Y that is not contained in past values of variable Y and other relevant information. Should past values of variable X contain information about current values of variable Y beyond the information contained in the Y sequence and the other variables in the information set, variable X is said to 'Granger cause' variable Y. The detection of Granger causality does not necessarily imply the presence of a physical causal mechanism between the two variables. Furthermore, the detection of Granger causality depends on the information set of conditioning variables. The coefficient estimates may be biased by the omission of relevant variables that are in fact the causal variables.

Here we look for an anthropogenic influence on global temperature by testing the ability of forcing variables such as trace gas concentrations and sulphate aerosols to explain a detected direction of Granger causality from Southern Hemisphere to Northern Hemisphere temperatures in a model that excludes those former variables. We find that the apparent dependence of Northern Hemisphere on Southern Hemisphere temperatures has strengthened over time and that the best explanation for this pattern is the influence of both anthropogenic trace gases and sulphate aerosols in addition to natural stratospheric sulphates and solar irradiance. To validate this result, we examine the temperature data generated by the Hadley Centre climate model (HCCM) when driven by atmospheres that are consistent with, and different from, the historical record. We find that the presence and direction of causal order is consistent with our hypothesis that the spatiotemporal pattern of greenhouse gases and tropospheric sulphates is responsible for the causal order found in the historical record.

South-to-north causal order

We first look for a causal order between the temperature series in a bivariate autoregressive model—equations (1) and (2). This type of model is known as a vector autoregression in the econometrics literature[17]. The test for causality is performed in two steps. In the first step, unrestricted and restricted forms of an equation are estimated. In the second step, a test statistic is calculated to test whether the restriction is binding. We illustrate this procedure by outlining the steps used to test the hypothesis that temperature in the Southern Hemisphere does not Granger cause temperature in the Northern Hemisphere. In the first step, we estimate the unrestricted model, which is given by equations (1) and (2) (which constitute model 1):

$$N_t = \alpha_1 + \beta_1 \, \text{time} + \sum_{i=1}^{s} \delta_{1i} N_{t-i} + \sum_{i=1}^{s} \phi_{1i} S_{t-i} + \epsilon_{1t} \qquad (1)$$

$$S_t = \alpha_2 + \beta_2 \, \text{time} + \sum_{i=1}^{s} \delta_{2i} N_{t-i} + \sum_{i=1}^{s} \phi_{2i} S_{t-i} + \epsilon_{2t} \qquad (2)$$

in which N_t is the temperature anomaly in the Northern Hemisphere[1,18,19], S_t is the temperature anomaly in the Southern Hemisphere[1,18,19], ϵ_t is a normally distributed random error term, and α_j, β_j, ϕ_{ji} and δ_{ji} are regression coefficients. The constant and time trend are included because univariate tests[20,21] indicate that the temperature data contain a deterministic trend.

The maximum number of lags, s, that we consider is $5 \approx T^{1/3}$, where T is the number of observations. A likelihood ratio test developed by Sims[17] indicates that s can be reduced to 4 without loss of explanatory power. The same result is indicated by the Akaike information criterion[22]—a likelihood-based goodness-of-fit criterion. These tests and sensitivity analyses are performed on the longest possible sample period that can support five lags—1865 to 1994. The earliest observation in our sulphur emission series is 1860.

We test for Granger causality by testing the significance of parametric restrictions in equations (1) and (2). We test whether Southern Hemisphere temperatures Granger cause temperature in the Northern Hemisphere by jointly restricting the ϕ_{1i} to zero thus excluding the lagged values of Southern Hemisphere temperatures from equation (1).

The significance of this restriction is evaluated by the test statistic ω:

$$\omega = \frac{(\text{RSS}_r - \text{RSS}_u)/s}{(\text{RSS}_u)/(T-k)} \qquad (3)$$

where T is the number of observations, k is the number of regressors in the unrestricted version of equation (1), s corresponds to the number of coefficients restricted to zero, RSS_r is the residual sum of squares from the restricted version of equation (1) and RSS_u is the residual sum of squares from the unrestricted version of equation (1). The test statistic ω is distributed with the F distribution with s and $(T-k)$ degrees of freedom in the numerator and denominator, respectively, under the assumption that the data series are stationary around a deterministic trend. Values of ω that exceed the critical value indicate that the residual sum of squares for the restricted model increases in a manner that is statistically significant (at the relevant level of significance, $p(F)$) relative to the residual sum of squares for the unrestricted model, in which case we reject the hypothesis of no causal order. To test whether Northern Hemisphere temperatures Granger cause Southern Hemisphere temperatures, we jointly restrict the δ_{2i} to zero, thus excluding the lagged values of Northern Hemisphere temperatures from equation (2).

The results indicate that temperature in the Northern Hemisphere does not Granger cause temperature in the Southern Hemisphere ($\omega(4) = 0.42$, $p < 0.79$). On the other hand, the results indicate that temperature in the Southern Hemisphere does Granger cause temperature in the Northern Hemisphere ($\omega(4) = 3.19$, $p < 0.016$).

If the data series are not trend-stationary but instead contain a random-walk component, the ω statistic cannot be evaluated against the F distribution. This type of non-stationarity is referred to in the econometric literature as the presence of a 'unit root'[23]. Univariate tests for this type of non-stationarity[20,21,24] indicate that the temperature anomalies for the Northern and Southern hemispheres are trend-stationary, and therefore the significance of the ω statistic can be evaluated with the standard F distribution.

The conclusion that the temperature data are trend-stationary is contradicted by results generated by preliminary analyses using multivariate techniques[25,26]. If greenhouse gases and other forcing factors that are known to contain unit roots drive temperature, the temperature series must contain this unit-root signal. The Dickey–Fuller and other unit-root tests tend to reject the null hypothesis too often when the data-generating process is a random walk with noise

and the noise is large relative to the signal[23,27]. In the multivariate setting, this noise is reduced and the signal is revealed. Even if the temperature data have a unit root, the significance of the test statistic ω can be evaluated with the F distribution if the data are cointegrated. Cointegration implies that the random-walk processes present in the two series are the same stochastic process. Under these conditions, there is a linear combination of the two variables that is stationary and to which the usual distribution theory can be applied.

If the data for temperature have a unit root and are not co-integrated, the presence of Granger causality cannot be tested accurately using the F distribution: evaluating ω against the F distribution would overstate its statistical significance[28,29]. This bias would cause us to argue for causality when none is present.

To analyse the distribution of the ω statistic if the temperature data are non-stationary and not cointegrated, we generated 1,000 experimental data sets each with 134 observations for temperature in the Northern and Southern Hemisphere. The model for each temperature series is a random walk with drift:

$$S_t = a_1 + S_{t-1} + e_{1t} \qquad (4)$$

$$N_t = a_2 + N_{t-1} + e_{2t} \qquad (5)$$

The model is calibrated by regressing the observed data on a constant and time trend and using the estimated regression coefficients for the time trend for a_1 and a_2 and the estimated error variances for the variances of e_{1t} and e_{2t}. The test statistic ω in equation (3) is calculated for each data set and these values are ranked in descending order. This ranking is used to evaluate the significance level (p(unit root)) of the test statistics using the simulated distribution. The value in position 50, which corresponds to the 0.05 critical value, is 3.01. The 5% critical value for the F distribution with 4 and 120 degrees of freedom, which is 2.44, is found at position 81, which corresponds to a significance level of 0.081.

The conclusion that Southern Hemisphere temperature 'Granger causes' Northern Hemisphere temperature remains, regardless of the presence of a unit root in the temperature data, when we evaluate the ω statistic against the distribution generated by the experimental data sets ($P < 0.04$).

Explanatory variables

By itself, the south-to-north causal order cannot be used to detect the effect of anthropogenic activities because the causal order may be generated by natural and/or anthropogenic mechanisms. To differentiate between these possibilities, we conduct several tests.

The south-to-north causal order might be generated by episodic, short-run, El Niño/Southern Oscillation (ENSO) teleconnections[30]. We evaluate this mechanism by analysing the causal order of temperature data averaged over periods thought to be longer than the ENSO teleconnections. If ENSO teleconnections generate the south-to-north causal order, the causal order should not be present in data averaged over long periods. The south-to-north causal order is present in temperature data averaged over the previous 5 years ($\omega(3) = 6.21, p < 5.95 \times 10^{-4}$), 10 years ($\omega(6) = 3.64, p < 0.003$), and 15 years ($\omega(6) = 3.84, p < 0.002$).

To explore the effects of other natural and anthropogenic mechanisms, we repeat the tests of Granger causality with models 2–5 that include natural and/or anthropogenic variables (Box 1). Expanding the model is necessary because we know that model 1 is mis-specified—it omits natural and/or anthropogenic variables that may affect temperature. This omitted-variable bias may generate the Granger causality described in the previous section. When the relevant natural and/or anthropogenic variables are included, this information may weaken or eliminate the change in the residual sum of squares that signals Granger causality.

To investigate the effect of natural and anthropogenic factors, we expand equation (1) to include exogenous variables:

$$N_t = \alpha_1 + \beta_1 \, \text{time} + \sum_{i=1}^{s} \delta_{1i} N_{t-i} + \sum_{i=1}^{s} \phi_{1i} S_{t-i}$$

$$+ \sum_{j=1}^{k} \sum_{i=1}^{s} \Gamma_{ji} Z_{jt-1} + \epsilon_{1t}$$

(6)

in which Z_{jt-i} are vectors of lagged values of exogenous variables and Γ_{ji} are regression coefficients. The time-series properties of the exogenous variables may affect the distribution of the test statistic. The distribution is unaffected by the addition of random walks if the temperature data are trend-stationary[28]. But if the temperature data contain a unit root, the distribution depends on the number of non-stationary variables added to the model. Univariate tests indicate that the radiative forcing of solar activity, anthropogenic emissions of sulphur, and the atmospheric concentrations of carbon dioxide,

---

Box 1 Models tested

Model 1. Temperature only

$$\text{Temp} = \alpha + \beta\text{time} + \sum_{t=1}^{k} \delta_t N_t + \sum_{t=1}^{k} \phi_t S_t$$

Model 2. Natural variables

$$\text{Temp} = \alpha + \beta \, \text{time} + \sum_{i=1}^{s} \delta_i N_{t-i} + \sum_{i=1}^{s} \phi_i S_{t-i}$$

$$+ \sum_{i=1}^{s} \Gamma_{1i} \text{Sun}_{t-i} + \sum_{i=1}^{s} \Gamma_{2i} \text{SSN}_{t-i} + \sum_{i=1}^{s} \Gamma_{3i} \text{SSS}_{t-i}$$

Model 3. Greenhouse gases

$$\text{Temp} = \alpha + \beta\text{time} + \sum_{i=1}^{s} \delta_i N_{t-i} + \sum_{i=1}^{s} \phi_i S_{t-i} + \sum_{i=1}^{s} \Gamma_{1i} \text{Sun}_{t-i} + \sum_{i=1}^{s} \Gamma_{2i} \text{SSN}_{t-i}$$

$$+ \sum_{i=1}^{s} \Gamma_{3i} \text{SSS}_{t-i} + \sum_{i=1}^{s} \Gamma_{4i} \text{CO2}_{t-i} + \sum_{i=1}^{s} \Gamma_{5i} \text{CH4}_{t-i}$$

$$+ \sum_{i=1}^{s} \Gamma_{6i} (\text{CFC11}_{t-i} + \text{CFC12}_{t-i} + \text{N2O}_{t-i})$$

Model 4. Tropospheric sulphates

$$\text{Temp} = \alpha + \beta\text{time} + \sum_{i=1}^{s} \delta_i N_{t-i} + \sum_{i=1}^{s} \phi_i S_{t-i} + \sum_{i=1}^{s} \Gamma_{1i} \text{Sun}_{t-i}$$

$$+ \sum_{i=1}^{s} \Gamma_{2i} \text{SSN}_{t-i} + \sum_{i=1}^{s} \Gamma_{3i} \text{SSS}_{t-i} + \sum_{i=1}^{s} \Gamma_{7i} \text{SOX}_{t-i}$$

Model 5. Greenhouse gases and tropospheric sulphates

$$\text{Temp} = \alpha + \beta\text{time} + \sum_{i=1}^{s} \delta_i N_{t-i} + \sum_{i=1}^{s} \phi_i S_{t-i} + \sum_{i=1}^{s} \Gamma_{1i} \text{Sun}_{t-i} + \sum_{i=1}^{s} \Gamma_{2i} \text{SSN}_{t-i}$$

$$+ \sum_{i=1}^{s} \Gamma_{3i} \text{SSS}_{t-i} + \sum_{i=1}^{s} \Gamma_{4i} \text{CO2}_{t-i} + \sum_{i=1}^{s} \Gamma_{5i} \text{CH4}_{t-i}$$

$$+ \sum_{i=1}^{s} \Gamma_{6i} (\text{CFC11}_{t-i} + \text{CFC12}_{t-i} + \text{N2O}_{t-i}) + \sum_{i=1}^{s} \Gamma_{7i} \text{SOX}_{t-i}$$

The symbols used above have meanings as follows: CFC11, radiative forcing of CFC11 (W m^{-2}; refs 40, 41); CFC12, radiative forcing of CFC12 (W m^{-2}; refs 40, 41); CH4, radiative forcing of methane (W m^{-2}; refs 42–45); CO2, radiative forcing of carbon dioxide (W m^{-2}; refs 46, 47); N, temperature anomaly in the Northern Hemisphere (°C; refs 1, 18, 19); N2O, radiative forcing of nitrous oxide (W m^{-2}; refs 48–50); S, temperature anomaly in the Southern Hemisphere (°C; refs 1, 18, 19); SOX, radiative forcing due to anthropogenic emissions of sulphates (W m^{-2}; ref. 51); SSN, radiative forcing due to stratospheric sulphates, Northern Hemisphere (W m^{-2}; ref. 52); SSS, radiative forcing due to stratospheric sulphates, Southern Hemisphere (W m^{-2}; ref. 52); Sun, solar activity (W m^{-2}; ref. 15); Temp, Temperature anomalies Northern or Southern Hemisphere (°C; refs 1, 18, 19). Greek characters are regression coefficients. The subscripts associated with equations for the Northern and Southern Hemisphere (equations (1) and (2)) are suppressed.

Radiative forcing is calculated from atmospheric concentration using the equations in Shine *et al.*[53] and Kattenberg *et al.*[54]; radiative forcing for CFCs accounts for the effect of ozone depletion, and the radiative forcing for nitrous oxide accounts for overlap with methane.

Table 1 Tests of Granger causality

	Lags	ω	p (F)	p (unit root)
Historical record				
Model 1 $\bar{R}^2 = 0.64416$				
North causes south	4	0.42	0.79	0.843
South causes north	4	**3.19**	0.016	0.039
Model 2 $\bar{R}^2 = 0.65674$				
North causes south	4	0.74	0.57	0.645
South causes north	4	**3.33**	0.013	0.027
Model 3 $\bar{R}^3 = 0.68989$				
North causes south	4	0.27	0.14	0.925
South causes north	4	2.14	0.081	0.151
Model 4 $\bar{R}^2 = 0.65211$				
North causes south	4	0.55	0.70	0.764
South causes north	4	**3.50**	0.010	0.028
Model 5 $\bar{R}^2 = 0.68599$				
North causes south	4	0.37	0.83	0.867
South causes north	4	1.87	0.12	0.206
HCCM experiments				
GHG 1861–1990				
North causes south	1	0.22	0.88	0.742
South causes north	1	2.74	0.10	0.247
SUL 1861–1990				
North causes south	1	0.01	0.91	0.932
South causes north	1	3.63	0.06	0.172
GHG 1991–2099				
North causes south	1	**4.70**	0.03	0.115
South causes north	1	1.75	0.19	0.353
SUL 1991–2099				
North causes south	1	**5.03**	0.02	0.093
South causes north	1	1.38	0.24	0.407

ω is as defined in equation (3), p(F) is the significance level using the F distribution, and p (unit root) is the significance level using our simulated unit root distribution.
In the 'historical record' data above, $\bar{R}^2$ indicates the adjusted R^2 value; two alternative hypotheses are tested for each model, 1–5. HCCM indicates Hadley Centre climate model (see text). Values that exceed the 0.05 threshold for statistical significance are shown in bold.

Table 2 Sensitivity analysis

Test no.	Change relative to base models				Model 1		Model 5	
	1864	Aggregate GHGS	5 lags	Contemporaneous effects	ω	p(F)	ω	p(F)
1	✔				**2.44**	0.011	2.31	0.063
2		✔			**3.19**	0.016	2.40	0.055
3			✔		**2.61**	0.028	0.95	0.45
4				✔	**3.19**	0.016	1.37	0.24
5	✔	✔			**3.44**	0.011	**2.95**	0.024
6	✔			✔	**3.44**	0.011	2.12	0.085
7			✔	✔	**2.61**	0.028	1.84	0.11
8		✔		✔	**3.19**	0.016	**2.68**	0.036
9			✔	✔	**2.61**	0.028	1.15	0.34
10		✔	✔	✔	**2.61**	0.028	**2.37**	0.046
11	✔	✔	✔	✔	**3.44**	0.011	**3.18**	0.017

Values that exceed the 0.05 threshold for statistical significance are shown in bold. Tick marks indicate change relative to base models.

methane, CFC11 (CCl_3F), CFC12 (CCl_2F_2) and nitrous oxide contain a unit root. We repeat the Monte Carlo simulations to estimate the distribution of the test statistic for models 2–5 in which the number of random walks is equal to the number of non-stationary variables in the Z vector. As before, the critical levels of the test statistic are increased.

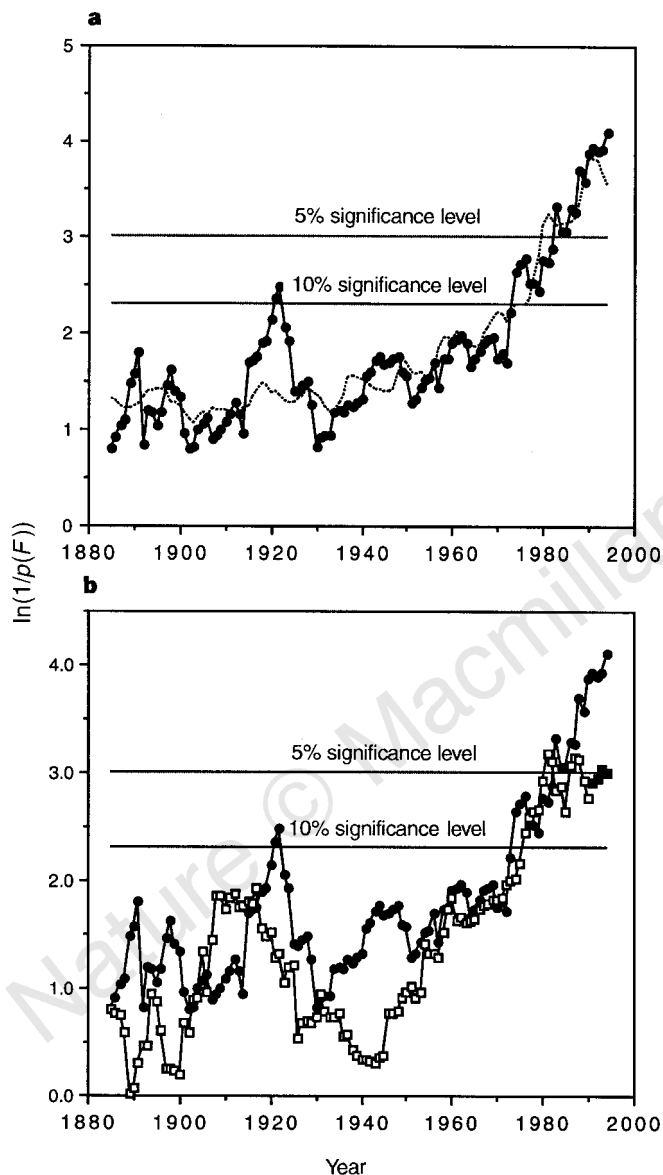The results of model 2 indicate that solar activity and the radiative

Figure 1 a, Changes in the statistical significance of the south-to-north causal order over time (filled circles). This is represented by the natural logarithm of the reciprocal of the significance level for tests carried out on subsamples ending at the dates indicated. The natural logarithm is used because the significance level is bounded from below by zero. The dotted line is the predicted value for ln(1/ significance level) based on the following equation that is fitted using ordinary least squares: $\ln(1/p(F)) = 1.36 - (1.07\,\text{RFSOX}) + (1.894\,\text{ORF}) - 0.026\,\text{year}$, where RFSOX is the radiative forcing of sulphates, ORF is the radiative forcing associated with greenhouse gases (CO_2, CH_4, CFCs and N_2O) and solar radiation, and 'year' is indexed to one in 1860. In **b**, the filled circles are the same variable as in **a**. Open squares are $\ln(1/p(F))$ of the same test on the data from the Hadley Centre SUL experiment (see text) simulated using historical estimates of sulphate aerosol for subsamples ending at the dates indicated. The filled squares are the same test extended to the end of 1994 using IPCC scenarios for greenhouse gases and sulphate aerosols.

forcing due to stratospheric sulphates do not affect the direction of causality indicated by model 1. Lagged values of temperature in the Southern Hemisphere contain statistically significant information about current values of temperature in the Northern Hemisphere ($\omega(4) = 3.33$, $p < 0.013$). This result also is significant when tested against the distribution generated with one random walk ($p < 0.027$).

Next we expand the vector of exogenous variables, Z, to also include the effects of anthropogenic activity. The results indicate that the south-to-north causal order is partially eliminated when the effect of greenhouse gases alone is included in model 3 (Table 1). The test statistic is significant at the 10% level but not at the 5% level. The null hypothesis cannot be rejected at the 10% significance level when tested against the distribution generated with four random walks ($p < 0.151$). Including the effect of sulphur emissions alone (model 4) does not reduce the statistical significance of the causal order in temperature (Table 1).

The results of model 5 indicate that the south-to-north causal order may be caused by both greenhouse gases and tropospheric sulphates. When these variables are included, the test statistic is insignificant as evaluated against a distribution generated with five random walks ($p < 0.206$) and the standard F distribution ($p < 0.12$).

Based on the lack of causal order in model 5 and the somewhat lesser reduction in the significance level in model 3, we hypothesize that the south-to-north causal order is generated by anthropogenic activities that increase the concentration of greenhouse gases globally, but which increase the concentration and effects of sulphate aerosols mainly in the Northern Hemisphere. We hypothesize that anthropogenic emissions of carbon dioxide, methane, CFCs and nitrous oxide increase radiative forcing globally because of their long residence time in the atmosphere. This tends to cause the temperature of the Earth to rise. This rise is retarded in the Northern Hemisphere by the presence of tropospheric sulphates. These aerosols spend a relatively short time in the atmosphere[31], and so their cooling effects are localized in the Northern Hemisphere.

Calculations indicate that the cooling effect of tropospheric sulphates in the Northern Hemisphere is larger than the heating effect of the higher concentration of greenhouse gases in the Northern Hemisphere relative to the Southern Hemisphere. One estimate for the total (both natural and anthropogenic) direct and indirect effect of sulphate aerosols in the Northern Hemisphere ($-0.72\,\text{W m}^{-2}$) is about two times greater than the negative effect of sulphate aerosols in the Southern Hemisphere ($-0.38\,\text{W m}^{-2}$)[32]. This $0.34\,\text{W m}^{-2}$ difference probably is much larger than the small difference in the radiative forcing of greenhouse gases in the Northern and Southern hemisphere, which is estimated to be about $2.1\,\text{W m}^{-2}$ globally. For example, the atmospheric concentration of carbon dioxide, CFC11 and CFC12 over the Northern Hemisphere is about 2–3% higher than over the Southern Hemisphere[33–36].

The hypothesis that the south-to-north causal order is generated by the spatiotemporal pattern of anthropogenic emissions of trace gases and sulphate aerosols is consistent with changes in the strength of the causal order over time. An iterative search indicates that the south-to-north causal order generally is not present in sample periods that start in 1865 and end before the 1970s, but is present in samples that start in 1865 and end later than the mid-1970s (Fig. 1a). This implies that anthropogenic variables may be responsible for the apparent direction of causality, though some sources of natural variability such as solar irradiance also have increased over this period[15]. The effect of anthropogenic activities is consistent with a simple model that indicates the significance level of the causal order is related to solar irradiance and the radiative forcing from greenhouse gases, and the radiative forcing associated with anthropogenic sulphur emissions (Fig. 1a). Standard tests such as the augmented Dickey–Fuller (-4.26) and the cointegrating Durbin–Watson (0.50) indicate that residuals from this

regression are stationary, which implies that the variables cointegrate and these two variables adequately model the non-stationarity in the significance level[37].

Sensitivity analysis

The relation between the south-to-north causal order and anthropogenic emissions of trace gases and sulphate aerosols also is consistent with the results of a sensitivity analysis in which model 1 and model 5 are estimated using alternative specifications. The alternative specifications include: (1) lengthening the sample period to include observations from 1864; (2) restricting the coefficients associated with the radiative forcing of each of the trace gases to be equal by aggregating their values; (3) increasing the number of lags to 5; and (4) including contemporaneous values of the explanatory variables in model 5. In addition, we examine combinations of these alternative specifications, which generates 11 possible tests (Table 2).

The sensitivity analysis confirms our general result—there is a statistically significant south-to-north causal order in model 1 that is reduced when information about the radiative forcing of trace gases and anthropogenic sulphate emissions are included in model 5. The south-to-north causal order of model 1 is present in all alternative specifications. The reduction in the statistical significance of the test in model 5 versus model 1 is reproduced in all specifications. Two of the alternative specifications, using five lags (test 3) and including contemporaneous effects (test 4) amplify our results by reducing greatly the significance level of the test statistic in model 5.

Cases in which the statistical significance of the south-to-north causal order remains above 5% in model 5 generally are associated with combinations of changes that aggregate the radiative forcing of greenhouse gases and extend the sample period to include observations from 1864. These alternative specifications are more restrictive than those used to generate the results in Table 1. Restricting the coefficients associated with the radiative forcing of individual gases to be equal is problematic, because there is some uncertainty about past levels of these gases and about the radiative forcing formulae, particularly in the case of ozone depletion due to CFCs; there are also differences between the effect on temperature of CO_2 and the other gases, due to possible effects of CO_2 on vegetation. The reliability of both the temperature and radiative-forcing data also declines as the sample is extended into the past.

Hadley Centre climate model

To test further the hypothesis that the south-to-north causal order is generated by anthropogenic emissions of greenhouse gases and tropospheric sulphates, we analyse temperature data generated by a coupled atmosphere–ocean general circulation model. If our hypothesis is correct, two results should emerge: (1) experiments run with atmospheres that emulate the historical concentration of greenhouse gases and tropospheric sulphates should reproduce the south-to-north causal order; and (2) a north-to-south or no causal order may be present when the CGCMs are simulated with atmospheres that have temporal and/or spatial concentrations of greenhouse gases and/or tropospheric sulphates that differ from the historical record.

We analyse results generated by the Hadley Centre climate model (HCCM) because it simulates three experiments that vary the spatial and temporal pattern of all greenhouse gases and tropospheric sulphates; the control experiment, the greenhouse gas (GHG) experiment, and the SUL experiment[38]. The control experiment holds constant the radiative forcing associated with greenhouse gases and tropospheric sulphates at a level consistent with their pre-industrial concentrations. The GHG experiments allows the radiative forcing of the atmosphere to increase at a rate consistent with the CO_2 equivalent of all greenhouse gases over the 1860–1990 historical period. The SUL experiment adds the effect of tropospheric sulphates to the effect of greenhouse gases.

The concentration of these gases in the 1991–2099 forecast horizon for the GHG and SUL experiments is derived from IPCC emission scenarios. The simulated atmospheres forecast a rapid increase in total radiative forcing associated with greenhouse gases, and a shift south towards the Equator in the spatial distribution of tropospheric sulphates.

The causal order of temperature data for the Northern and Southern Hemisphere found in the control, GHG and SUL experiments over the historical reconstructions and forecast horizons are consistent with the hypothesis that the south-to-north causal order in the historical record is generated by the atmospheric concentration of greenhouse gases and tropospheric sulphates. When the HCCM is simulated with an atmosphere that emulates radiative forcing associated with all greenhouse gases and tropospheric sulphates between 1860 and 1990 (the SUL experiment), applying the causality test to the simulation output suggests ($p < 0.06$) south-to-north causal order (Table 1). An iterative search shows that the strength of the causal order in the SUL experiment follows a pattern similar to the historical record—it generally strengthens over time (Fig. 1b). If the SUL experiment were re-run with historical data to the end of 1994, it may increase the significance level of the causal order in the SUL experiment in much the same way as extending the sample period for 1991 to 1994 increases the strength of the causal order in the historical record. Indeed, using the data for 1991–94 from the IPCC scenarios does increase the strength of the relation beyond the 0.05 threshold ($\omega(1) = 3.93, p < 0.049$). Nonetheless, the strength of the south-to-north causal order is weaker than that found in the historical record, and is less robust to changes in lag length than the results generated by the historical record. This is as would be expected, because the experiment did not simulate changes in variables such as solar activity and ozone depletion, and the model cannot be expected to simulate all aspects of the climate system accurately.

On the other hand, there is no causal order in historical temperature data when the HCCM is simulated with an atmosphere that allows radiative forcing to increase at a rate consistent with the CO_2 equivalent of all greenhouse gases over the 1860–1990 historical period but ignores changes in sulphate aerosols (GHG experiment). The results for the control scenario are uncertain. The dates in the control experiment have no connection to historical events, so we test all possible 130-year samples in the 1850–2099 period for which data are available from the control experiment against a distribution generated by the procedure described by Christiano[39]. Some periods show a south-to-north causal order if the data are stationary. Subsamples with the largest test statistics are significant at the 1% level. No periods show a causal order if the data are nonstationary as implied by univariate tests of the temperature difference between Northern and Southern Hemisphere: the largest test statistic is significant at the 14.1% level (that is, $p < 0.141$).

The temperature data show a strong north-to-south order over the 1991–2099 period when the HCCM is simulated with an atmosphere that is forced by emission of greenhouse gases and tropospheric sulphates given by the IPCC scenario (Table 1). The north-to-south causal order also is found when the model is simulated with an atmosphere forced only by the emission of greenhouse gases given by the IPCC scenario (Table 1).

We find that a south-to-north causal order is suggested by the data simulated by an atmosphere intended to reproduce the historical record, whereas it is not present or runs in the opposite direction in data from counterfactual simulations. This is consistent with the hypothesis that the south-to-north causal order is generated by the historical combination of greenhouse gases and tropospheric sulphates.

Conclusion

This analysis suggests that human activity has played a role in the historical record of temperature. The south-to-north causal order in

the historical temperature record may be a fingerprint of the spatial and temporal pattern of anthropogenic activities that emitted greenhouse gases and tropospheric sulphates between 1865 and 1994. Combined with other results, our results provide further evidence for the conclusion that "the observed trend in global mean temperature over the past 100 years is unlikely to be entirely natural in origin."[7]   □

1. Jones, P. D. Hemispheric surface air temperature variations: a reanalysis and an update to 1993. *J. Clim.* **7**, 1794–1802 (1994).
2. Vinnikov, K. Y., Groisman, P. Y. & Lugina, K. M. Empirical data on contemporary global climate changes (temperature and precipitation). *J. Clim.* **3**, 662–677 (1990).
3. Hansen, J. & Lebedeff, S. Global trends of measured air temperature. *J. Geophys. Res.* **92**, 13345–13372 (1987).
4. Kerr, R. A. Is the world warming or not. *Science* **267**, 612 (1995).
5. Schneider, S. H. Detecting climatic change signals: are there any fingerprints? *Science* **263**, 341–347 (1994).
6. Lindzen, R. S. Some coolness concerning global warming. *Bull. Am. Meteorol. Soc.* **71**, 288–299 (1990).
7. Santer, B. D., Wigley, T. M. L., Barnett, T. P. & Anyamba, E. in *Climate Change 1995: The Science of Climate Change* (eds Houghton, J. T. *et al.*) 407–433 (Cambridge Univ. Press, 1996).
8. Santer, B. D. *et al.* A search for human influences on the thermal structure of the atmosphere. *Nature* **382**, 39–46 (1996).
9. Lane, L. J., Nichols, M. H. & Osborn, H. B. Time series analysis of global change data. *Environ. Pollut.* **83**, 63–88 (1994).
10. Kuo, C., Lindberg, C. & Thomson, D. J. Coherence established between atmospheric carbon dioxide and global temperature. *Nature* **343**, 709–714 (1990).
11. Thomson, D. J. The seasons, global temperature, and precision. *Science* **268**, 59–68 (1995).
12. Schönwiese, C. D. Analysis and prediction of global climate temperature change based on multiforced observational statistics. *Environ. Pollut.* **83**, 149–154 (1994).
13. Tol, R. S. J. & de Vos, A. F. Greenhouse statistics–time series analysis. *Theor. Appl. Climatol.* **48**, 63–74 (1993).
14. Tol, R. S. J. Greenhouse statistics–time series analysis: Part II. *Theor. Appl. Climatol.* **49**, 91–102 (1994).
15. Lean, J. L., Beer, J. & Bradley, R. Reconstruction of solar irradiance since 1610: implications for climate change. *Geophys. Res. Lett.* **22**, 3195–3198 (1995).
16. Granger, C. W. J. Investigating causal relations by econometric models and cross spectral models. *Econometrica* **37**, 424–438 (1969).
17. Sims, C. Macroeconomics and reality. *Econometrica* **48**, 1–49 (1980).
18. Nicholls, N. *et al.* in *Climate Change 1995: The Science of Climate Change* (eds Houghton, J. T. *et al.*) 138–192 (Cambridge Univ. Press, 1996).
19. Parker, D. E., Jones, P. D., Folland, C. K. & Bevan, A. 1994. Interdecadal changes of surface temperatures since the late 19th century. *J. Geophys. Res.* **99**, 14373–14399 (1994).
20. Dickey, D. A. & Fuller, W. A. Distribution of the estimators for autoregressive time series with a unit root. *J. Am. Statist. Assoc.* **74**, 427–431 (1979).
21. Phillips, P. & Perron, P. Testing for a unit root in time series regression. *Biometrica* **75**, 335–346 (1988).
22. Akaike, H. in *2nd Int. Symp. on Information Theory* (eds Petrov, P. N. & Csaki, F.) 267–281 (Akadacemiai Kiadaco, Budapest, 1973).
23. Hamilton, J. D. *Time Series Analysis* (Princeton Univ. Press, 1994).
24. Schmidt, P. & Phillips, P. C. B. LM tests for a unit root in the presence of deterministic trends. *Oxford Bull. Econ. Statist.* **34**, 357–287 (1992).
25. Johansen, S. Statistical analysis of cointegration vectors. *J. Econ. Dynam. Control* **12**, 231–254 (1988).
26. Johansen, S. & Juselius, K. Maximum likelihood estimation and inference on cointegration with application to the demand for money. *Oxford Bull. Econ. Statist.* **52**, 169–209 (1990).
27. Enders, W. *Applied Econometric Time Series* (Wiley, New York, 1995).
28. Toda, H. Y. & Phillips, P. C. B. The spurious effects of unit roots on exogeneity tests in vector autoregressions: an analytic study. *J. Econometr.* **59**, 229–255 (1993).
29. Ohanian, L. E. The spurious effects of unit roots on vector autoregressions. *J. Econometr.* **39**, 251–266 (1988).
30. Philander, S. G. *El Nino, La Nina, and the Southern Oscillation* (Academic, San Diego, 1990).
31. Alkezweeny, A. J. Trend analyses of sulfur dioxide emissions and sulfate concentrations and their application for global cooling. *Atmósfera* **8**, 91–97 (1995).
32. Kiehl, J. T. & Briegleb, B. P. The relative roles of sulphate aerosols and greenhouse gases in climate forcing. *Science* **260**, 311–314 (1993).
33. Keeling, C. D. *et al.* in *Aspects of Climate Variability in the Pacific and Western Americas* (ed. Petersen, D. H.) 165–236 (Geophys. Monogr. 55, Am. Geophys. Un., Washington DC, 1989).
34. Siegenthaler, U. & Sarmiento, J. L. Atmospheric carbon dioxide and the ocean. *Nature* **365**, 119–125 (1993).
35. Faser, P. & Derek, N. in *Baseline 91* (eds Dick, C. & Gras, J.) 70–81 (Bureau of Meteorology-CSIRO, Melbourne, 1994).
36. Fraser, P., Penkett, S., Gunson, M., Weiss, R. & Rowland, F. S. in *Concentrations, Lifetimes, and Trends of CFC's Halons, and Related Species* (eds Kay, J, Penket, S. & Ormand, F.) 1.1–1.68 (Rep. No. 1339, NASA, Washington DC, 1994).
37. Engle, R. E. & Granger, C. W. J. Cointegration and error-correction: representation, estimation, and testing. *Econometrica* **55**, 251–276 (1987).
38. Mitchell, J. F. B., Johns, T. C., Gregory, J. M. & Tett, S. F. B. Climate response to increasing levels of greenhouse gases and sulphate aerosols. *Nature* **376**, 501–504 (1995).
39. Christiano, L. J. Searching for a break in GNP. *J. Bus. Econ. Statist.* **10**, 237–250 (1992).
40. Prather, M., McElroy, M., Wofsy, S., Russel, G. & Rind, D. Chemistry of the global troposphere: fluorocarbons as tracers of air motion. *J. Geophys. Res.* **92**, 6579–6613 (1987).
41. Elkins, J. W. *et al.* in *Trends '93: A Compendium of Data on Global Change* (eds Boden, T. A., Kaiser, D. P., Sepanski, R. J. & Stoss, F. S.) 501–504 (ORNL/CDIAC-65, Carbon Dioxide Information Analysis Center, Oak Ridge Natl Lab., Oak Ridge, TN, 1994).
42. Etheridge, D. M., Pearman, G. I. & Fraser, P. J. in *Trends '93: A Compendium of Data on Global Change* (eds Boden, T. A., Kaiser, D. P., Sepanski, R. J. & Stoss, F. S.) 256–260 (ORNL/CDIAC-65, Carbon Dioxide Information Analysis Center, Oak Ridge Natl Lab., Oak Ridge, TN, 1994).
43. Khalil, M. A. K. & Rasmussen, R. A. Global emissions of methane during the last several centuries. *Chemosphere* **29**, 833–842 (1994).
44. Dlugokenchy, E. J., Lang, P. M., Masarie, K. A. & Steele, L. P. in *Trends '93: A Compendium of Data on Global Change* (ORNL/CDIAC-65, Carbon Dioxide Information Analysis Center, Oak Ridge Natl Lab., Oak Ridge, TN, 1994).
45. Prinn, R. G. *et al. CDIAC World Data Center Dataset No. DB-1001* (Available by anonymous ftp from cdiac.esd@ornl.gov).
46. Etheridge, D. M. *et al.* Natural and anthropogenic changes in atmospheric CO_2 over the last 1,000 years from air in Antarctic ice and firn. *J. Geophys. Res.* **101**, 4115–4128 (1996).
47. Keeling, C. D. & Whorf, T. P. in *Trends '93: A Compendium of Data on Global Change* (eds Boden, T. A., Kaiser, D. P., Sepanski, R. J. & Stoss, F. S.) 16–26 (ORNL/CDIAC-65, Carbon Dioxide Information Analysis Center, Oak Ridge Natl Lab., Oak Ridge, TN, 1994).
48. Prinn, R. D. *et al.* Atmospheric emissions and trends of nitrous oxide deduced from ten years of ALE/GAGE data. *J. Geophys. Res.* **95**, 18369–18385 (1990).
49. Prinn, R. D. *et al. CDIAC World Data Center Dataset No. DB-1001* (Oak Ridge, 1995).
50. Machida, T., Nakazawa, T., Fujii, Y., Aooki, A. & Watanabe, O. Increase in the atmospheric nitrous oxide concentration during the last 250 years. *Geophys. Res. Lett.* **22**, 2921–2924 (1995).
51. Stern, D. I. & Kaufmann, R. K. *Estimates of Global Anthropogenic Sulfate Emissions 1860–1993* (Working Paper 9602, Centre for Energy & Environmental Studies, Boston University, 1996); (available at http://cres.anu.edu.au/~dstern/CEES_WP/9602.w)
52. Sato, M., Hansen, J. E., McCormick, D. J. & Pollack, J. B. Stratospheric aerosol optical depths, 1850–1990. *J. Geophys. Res.* **98**, 22987–2294 (1993).
53. Shine, K. P. R. G., Derwent, D. J., Wuebbles, D. J. & Mocrette, J. J. in *Climate Change: The IPCC Scientific Assessment* (eds Houghton, J. T., Jenkins, G. J. & Ephramus, J. J.) 47–68 (Cambridge Univ. Press, 1991).
54. Kattenberg, A. F. *et al.* in *Climate Change 1995: The Science of Climate Change* (eds Houghton, J. T. *et al.*) 289–357 (Cambridge Univ. Press, 1996).